Crystallization Behavior of Ultrahigh Molecular Weight Polyethylene as a Function of in Vacuo γ-Irradiation

Saša Andjelić*,† and Robert E. Richard‡

Ethicon, Inc., a Johnson & Johnson Company, P.O. Box 151, Somerville, New Jersey 08876-0151, and DePuy Orthopaedics, Inc., a Johnson & Johnson Company, P.O. Box 988, Warsaw, Indiana 46581-0988

Received May 15, 2000; Revised Manuscript Received December 18, 2000

ABSTRACT: A comprehensive investigation was carried out to study the effects of in vacuo γ-irradiation on the crystallization behavior of ultrahigh molecular weight polyethylene (UHMWPE) used in joint replacement prostheses. A wide variety of experimental techniques, including differential scanning calorimetry (DSC), wide-angle X-ray diffraction (WAXD), synchrotron small-angle X-ray scattering (SAXS), hot stage optical microscopy (HSOM), and depolarized light scattering (DLS), was used to access information about lamellar and supramolecular morphology, degree of crystallization, and crystallization kinetics during different nonisothermal and isothermal procedures. It was found that network formation prevailed over chain scission processes in the in vacuo irradiated samples, lowering the crystallizability of the polymer due to imposed geometrical constrains. In addition, the physical net of stable entanglements accompanied by the extensive cross-linking produced by γ-irradiation generated quite unique crystallization morphology of UHMWPE. We detected the presence of distinct ordered grains, whose size depended on the irradiation dose, that did not "melt" even after being subjected to a high-temperature heating cycle. At lower temperatures, however, progressive chainlike nucleation proceeded right on the skirt of these domains, maintaining the constant crystallization rate regardless of the degree of undercooling.

Introduction

Ultrahigh molecular weight polyethylene (UHMWPE) has been the material of choice for use as a bearing material in total joint replacements (TJR) for some time due to its unique and unmatchable physical and mechanical properties. Very high molecular weight and long relaxation time of UHMWPE chains provide a structural foundation for superior toughness and resistance to creep and wear. Nonetheless, it is still viewed as the weak link in total joint replacement systems. The UHMWPE particulate matter that is produced as the result of articulation of these bearings with associated metal components can result in osteolysis of the surrounding bone. The clinical result is a reduced lifetime of the total joint due to weakening of the fixation, resulting in implant loosening and failure.[1]

It has been shown that the mode of sterilization of UHMWPE bearings can strongly influence the degree of wear in TJRs.[2−5] Until recently, a majority of UHMWPE bearings were sterilized by γ-radiation in an air atmosphere at a nominal dose of 2.5 Mrad. The orthopaedic industry has since learned that this practice leads to the generation of free radical species due to homolytic bond cleavage. If these free radicals react with each other in an intermolecular manner on the UHMWPE backbone, then cross-links are formed which impart an improved wear resistance to the bearing. If, however, they react with oxygen present in the packaging atmosphere during shelf storage, then oxidation of the bearings will occur. Furthermore, bearings that remain in air for extended periods of time prior to implantation can oxidize to the extent that they are more predisposed to failure once implanted.

Recent developments in the sterilization of UHMWPE bearings such as the use of gas plasma or ethylene oxide have been implemented to address this oxidation problem.[2] However, nonirradiation modes of sterilization do not produce the beneficial cross-linking that results in the improvement of wear properties. A more effective way of addressing this sterilization issue has been to alter the packaging of orthopaedic bearing to allow the γ-sterilization to be conducted in an oxygen-free environment. Examples of this include the γ-sterilization and packaging using vacuum or barrier packaging technology.[4] While this approach solves the problem of oxidation during shelf storage, the free radicals are still present and may react in vivo to reduce the lifetime of the bearing.

In the past 2 years, a new generation of UHMWPE bearings has been commercialized by a number of major orthopaedic implant companies.[4,5] These devices have shown an order of magnitude improvement in wear properties compared to previous generations of UHMWPE bearings. These products are made by exposing UHMWPE raw materials to irradiation doses in the range of 5−10 Mrad to generate high concentrations of free radicals, followed by a thermal treatment at temperatures approaching or above the melting point which leads to extensive cross-linking. In addition to the greatly improved wear properties, these products are virtually free of radical species providing a highly stable product.

The objective of the present work is to study the effect that the extensive network formation produced by γ-irradiation in a vacuum has on the crystallization behavior of UHMWPE. A wide variety of experimental techniques was used to access information about lamellar and supramolecular morphology, degree of crystallization, and crystallization kinetics during different nonisothermal and isothermal conditions. To the best of our knowledge, this is the first time that crystalliza-

† Ethicon, Inc.
‡ DePuy Orthopaedics, Inc.
* To whom correspondence should be addressed.

10.1021/ma0008241 CCC: $20.00
Published on Web 01/18/2001

Table 1. Irradiation History of UHMWPE

name	$M_v \times 10^6$ (g/mol)	irradiation dose (KGy)	swell ratio, q	M_c (g/mol)
1050[a]	6	0	N/A[b]	N/A
1050-0	6	0	N/A	N/A
1050-10	6	10	6.20	20000
1050-50	6	50	3.00	6200
1050-100	6	100	2.40	4000
1020[a]	3	0	N/A	N/A
1020-0	3	0	N/A	N/A
1020-10	3	10	7.20	25000
1020-50	3	50	3.40	7800
1020-100	3	100	3.00	6200

[a] As-received samples; underwent no thermal treatment (at 155 °C for 24 h). [b] N/A = not applicable.

tion kinetics of UHMWPE has been analyzed as a function of γ-irradiation.

Experimental Section

Materials. The UHMWPE used in this study consisted of GUR 1020 and GUR 1050 grades available from Ticona, Bayport, TX. Both polymers were consolidated into 3 in. bar stock using ram extrusion processing. The 1050 based product was produced by Poly Hi Solidur (Ft. Wayne, IN), and the 1020 was produced by Perplas Medical Limited (Bacup, England). Samples with reported viscosity average molecular weights of about 3 and 6 million were studied with intrinsic viscosities of 20 and 30 dL/g, respectively. The density of both materials was found to be 0.932 g/cm^3. No additional stabilizers or processing aids have been used in fabricating the materials. The polymer in fabricated form was free of residual particles larger than 300 μm in diameter. Molecular weight distributions of virgin samples were described elsewhere.[6]

Irradiation/Heat Treatment Procedure. Each sample consisted of 3 in. long pieces of bar stock. The samples were vacuum packaged in aluminum-coated heat-sealable pouches. They were γ-irradiated at room temperature with a cobalt-60 source at the nominal doses of 10, 50, and 100 KGy at Steris Isomedix, Whippany, NJ. The subsequent thermal treatment consisted of heating the samples to 155 °C in a vacuum oven for 24 h.

Molecular Weight between Cross-Links. The molecular weight between cross-links (M_c) was determined from swell ratio data according to ASTM D2765. In short, a carefully weighed polymer is immersed into solvent, *o*-xylene, which is boiled vigorously enough (140 °C) to ensure good agitation of the solution. After the extraction of polymer (for about 12 h), the specimen was dried in the vacuum oven at 150 °C, until it reached the constant weight. The swell ratio, the ratio of the gel volume in the swollen state to its volume in the unswollen state, was used then to determine the network chain density (ν^*) and M_c according to the theory of Flory and Rehner[7] using eqs 1 and 2:

$$\nu^* = -[\ln(1 - q^{-1}) + q^{-1} + Xq^{-2}/V_1(q^{-1/3} - 0.5q^{-1})] \quad (1)$$

and

$$M_c = 1/\nu^* V_1 \quad (2)$$

where q is the swell ratio, X is the Flory interaction parameter, and V_1 is the molar volume of the swelling solvent, *o*-xylene. A summary of these results is presented in Table 1. The swell ratio and the molecular weight between cross-links decreased with an increase in irradiation dose. Slightly higher values of q and M_c were observed for the lower molecular weight series.

Techniques. *Differential Scanning Calorimetry (DSC).* DSC measurements were performed with a TA Instruments differential scanning calorimeter, model 2910 MDSC, using dry N_2 as a purge gas. The instrument was calibrated with an indium standard for temperature and heat change. An empty aluminum pan was used as reference. Calorimetric measurements were conducted in three ways: (1) from room temperature, the sample was heated under a constant heating rate of 10 °C/min; (2) after melting, the sample was cooled under a controlled rate; (3) after melting, the sample was rapidly cooled to a temperature of interest and the crystallization measured under these isothermal conditions.

The experiments on the isothermal melt crystallization of UHMWPE were carried out as follows: a sample of about 4 mg was first melted and maintained for 5 min at 200 °C (60 °C above its melting point). Subsequently, tested materials were rapidly cooled (ca. 50 °C/min) to the constant test (crystallization) temperature. Crystallization behavior was characterized over the temperature range between 110 and 124 °C. The isothermal heat flow curves were integrated to determine the crystallinity as a function of time. The crystallinity, X_c of the samples were calculated using the following formula

$$X_c = \frac{\Delta h}{\Delta h_{100}} \times 100 \quad (3)$$

where Δh is heat of crystallization of the sample and Δh_{100} is the heat of crystallization for a 100% crystalline sample taken as 289 J/g.[8]

Hot Stage Optical Microscopy (HSOM). The optical hot stage experiments were conducted using a Mettler FP90 central processor with a Mettler FP82HT hot stage to control sample conditions. Nitrogen flow for cooling the stage was regulated with a Dwyer (0−50 scfm) flowmeter. The hot stage was mounted on a Nikon SMZ-U microscope equipped with a 1× objective and a 1:10 zoom. Images from the microscope were obtained using a Microimage i308 low light integrating video camera. The digital images were captured and analyzed using Image Pro Plus (Version 4.0) imaging software. Further experimental details of HSOM are described elsewhere.[9]

Prior to the HSOM measurement, each sample was precisely microtomed to the uniform thickness of 0.10 mm (0.25 mm) with the maximum error of less than 2%. During measurements specimens were held perfectly parallel by the hot stage unit preventing any change of samples' dimension.

Depolarized Light Scattering (DLS). A 20 mW HeNe laser (Uniphase, Manteca, CA) with $\lambda = 0.633$ μm was used as the light source for small-angle depolarized light scattering. The light was directed through an uncoated right-angle glass prism, followed by the compensator (quartz quarter-wave retardation plate) and the first polarizer. The laser beam then reached the sample, which was enclosed in the optical Linkam CSS 450 Cambridge Shearing System (Linkam Scientific Instruments Ltd., Tadworth, Surrey, UK) supplied with a precise temperature control unit. The light emerging from the sample passed through a broad-band beam sampler (splitter), where approximately 5% of the light was redirected and focused onto a silicon photodiode. This diode detector measures changes of the total light intensity before and after crystallization was initiated. The major portion of the light beam, unaffected by the sampler, advanced to the second polarizer (analyzer). From there, the final scattering pattern was projected onto a high-quality paper screen using a 50 mm dielectric mirror.

Coordinates in the projection plane are determined by two angles, θ and μ. The scattering vector q, defined as $q = 4\pi/\lambda \sin(\theta/2)$, was calibrated using the four concentric circles method as described elsewhere.[10] The scattering profiles were recorded by a NEC TI-324A CCD industrial high-resolution monochrome camera, equipped with a Nikon 28 mm lens and positioned on the optical rails. The distance between the screen and camera system was kept at 16 cm during all real-time measurements. The digital images were captured and analyzed using Image Pro Plus (Version 4.0) imaging software. The entire set up was mounted on a research grade optical table supported by vibrational isolators.

Wide-Angle X-ray Diffraction (WAXD). Supporting data on the crystallization behavior of UHMWPE were obtained from WAXD. The X-ray measurements of irradiated and nonirra-

Table 2. DSC Crystallization Properties of UHMWPE Obtained during the First Heating Run with the Heating Rate of 10 °C/min; WAXD Data Generated on the Same Samples Are Included as Well

name	H_m (J/g)	T_m (°C)	X_c[a] (%)	α[b] (%)
1050	141.5	137.5	49.0	47.0
1050-0	149.0	138.5	51.5	48.0
1050-10	123.5	137.0	43.0	45.0
1050-50	115.0	137.5	40.0	43.0
1050-100	115.5	141.0	40.0	44.0
1020	145.0	138.0	50.0	52.0
1020-0	150.5	139.5	52.0	51.0
1020-10	128.5	139.0	44.5	48.0
1020-50	122.0	137.5	42.5	45.0
1020-100	116.5	139.0	40.5	44.0

[a] Percent of crystallinity based on H_m (100%) = 289 J/g.[8] [b] Percent of crystallinity determined from wide-angle X-ray diffraction (WAXD).

diated films were carried out on a Siemens Hi-Star unit using Cu Kα radiation at the wavelength of 1.542 Å. The instrument was operated at 40 kV and 40 mA with a collimator diameter of 0.5 mm. Samples were mounted on the goniometer in such a way that the surface of a polymer film was positioned normal to the X-ray beam. The deconvolution of the X-ray images and the calculation of crystallinity content were conducted using the DIFFRAC PLUS software developed by Siemens.

Synchrotron Small-Angle X-ray Scattering (SAXS). Small-angle X-ray scattering patterns were obtained at the Advanced Polymers Beamline ($X3A_2$) in the National Synchrotron Light Source (NSLS), Brookhaven National Laboratory (BNL), New York. This beamline is controlled and operated by the New York State University at Stony Brook. The sample-to-detector distance was 1205 mm. The wavelength was 1.54 Å. Sample exposure time was 60 s. The SAXS patterns were recorded by means of a 2D imaging plate detector. The one-dimensional SAXS profile, once extracted from the 2D scattering pattern, can be analyzed via the method of correlation function for crystalline polymers. The theory of this approach and further details of the experimental procedure can be found in other recent studies.[11−13]

Results and Discussion

1. Effect of γ-Radiation on Thermal Behavior and Ultimate Crystallinity Content of UHMWPE Films. We begin our discussion by presenting the DSC data of various UHMWPE films collected during the first heating scan. Values of the heat of fusion, H_m, listed in the second column in Table 2, are directly related to the bulk crystallinity developed in the sample. With an increase in irradiation dose, H_m, and thus crystallinity, decreased regularly for both 1050 and 1020 samples. The biggest drop in the crystallinity was noticed after the lowest irradiation dose had been introduced (10 KGy). In general, for the same irradiation level used, a slight increase in the crystallinity for the lower molecular weight population (1020) was observed. Contrary to our findings, there are reports in the literature suggesting that the degree of crystallinity calculated from DSC methods for UHMWPE, in fact, increases with irradiation dose.[14−17] These studies indicated that the chain scission, followed by eased recrystallization of the new shorter segments, was the dominant effect produced by γ-irradiation rather than the cross-linking process. The visual effect of such irradiation mechanism was usually manifested by a color change from white to brownish caused by the oxidation process occurring instantly after the breakage of the chain backbone. It was found that this transition became more prominent with an increase in irradiation dose.[18] In the present study, however, we observed no change in the color of the polymer with irradiation. Since the UHMWPE samples were irradiated and stored in a vacuum package, the potential for oxidative degradation was minimized. In addition, all irradiated samples were subsequently heated above the melt to eliminate free radical species that have been associated with oxidative chain scission reactions. Finally, the mid-infrared spectroscopy revealed that no carbonyl or double-bond formation was detectable in any of our irradiated samples. These data lead us to believe that network formation in the in vacuo irradiated UHMWPE prevailed over chain scission, which, in turn, lowered the overall crystallinity achieved upon cooling and annealing due to imposed geometrical constrains. The melting temperatures (T_m) of the UHMWPE samples were found to be in the range of 137 and 141 °C with no apparent trend assigned as indicated in Table 2. Similarly, T_m values determined from the second heating run appeared to be independent of irradiation dose, but they were slightly lower (from 135 to 136.5 °C, not listed here). In some of the earlier studies, an increase in the melting temperature upon irradiation has been reported.[15,17] This was explained by thicker but more perfect lamellae produced by shorter unfolded chains originated from the cleavage process. It is worth mentioning that even for a virgin nonirradiated UHMWPE, a wide range of T_m values were reported throughout the literature. These differences could be rationalized by the specific kind of UHMWPE used and by the processing history of the sample.

Using DSC data from Table 2, the crystalline lamellar thickness, l_c, was estimated from the melting point of the polymer, T_m, via the Thomson−Gibbs equation:[19]

$$T_m = T_{m0}\left(1 - \frac{2\sigma_e}{l_c \Delta h}\right) \tag{4}$$

where T_{m0} = 418.7 K is the melting point for a hypothetical crystal of infinite size for which surface energy effects may be disregarded.[19] A value of 93×10^{-7} J/cm^2 was used for the fold surface energy, σ_e, which is related to the surface energy of the crystal end faces at which the chains fold. The heat of fusion of the crystal, Δh, was taken to be 289 J/g ≈ J/cm^3 (since the density of the crystalline phase is 1.005 g/cm^3).[8,20] Calculated values for l_c were in the range from 310 to 575 Å, depending on the melting temperatures. Larger lamellar thicknesses corresponded to higher melting temperatures, and vice versa. To gain further information about changes in crystal lamellar morphology of UHMWPE upon irradiation, synchrotron small-angle X-ray scattering (SAXS) measurements were conducted at Brookhaven National Laboratory. After examining all of our polymers, we found that their SAXS profiles could not be spatially resolved because of the limitation of the instrument. SAXS images of the nonirradiated (1050-0) and irradiated (1050-50) samples (not shown here) suggested that integration of the SAXS pattern was not possible since the anticipated scattering ring could not be distinguished from the intensity near the stop beam located at the center of images for both materials. Furthermore, from the location (diameter) of the center beam and other measuring parameters, including the sample-to-detector distance, we estimated that the long period thickness (sum of crystalline and amorphous layer thicknesses) could not fall in the range below 750−800 Å. To measure lamellar thicknesses

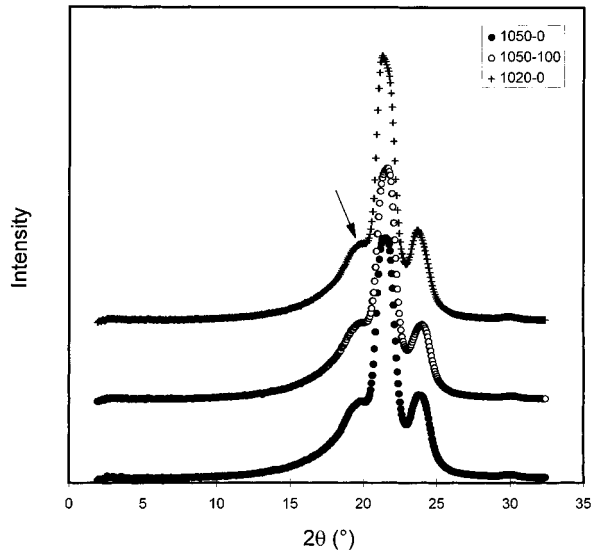

Figure 1. WAXD images of the three different UHMWPE. An arrow indicates a monoclinic structure peak located at $2\theta = 19.5°$, which originated from 001 plane diffraction. Two upper graphs were shifted vertically for clarity reasons.

greater than this range, one should have an access to the synchrotron ultrasmall X-ray scattering equipment. The fact that SAXS data might suggest thicker lamellae than what the DSC technique employed (for this material $L \sim 2l_c$) is intriguing and needs further explanation. We believe that incomplete melting of larger crystal structures found in our UHMWPE samples (discussed later in the text) directly influenced DSC results. Because of the possible presence of the nondisintegrated crystalline domains,[21] the location of DSC melting peak was shifted to lower temperatures as it lacked contribution of larger crystal lamellae still preserved in the melt. Similarly, Bellare et al.[22] reported that lamellar morphology of UHMWPE, examined by the SAXS method, contained a large distribution of lamellar thicknesses, diffuse interfaces, and a large variation of interlamellar spacing.

Wide-angle X-ray diffraction (WAXD) measurements were carried out to evaluate the crystal structure of the studied polymers. As indicated in Table 2, very good agreement exists between DSC and WAXD methods regarding the calculation of overall crystallinity content. The same trend that was discussed previously for the heat of fusion changes applies here as well. Integrated diffraction patterns of three different UHMWPE films are presented in Figure 1. The indexes of refraction [110] and [200], which correspond to the orthorhombic unit cell, are seen at $2\theta = 21.6°$ and 24.0°, respectively. One of the important features of these WAXD patterns is the presence of a substantial amount of monoclinic structure (i.e., [001] plane at $2\theta = 19.5°$, indicated by an arrow) observed in all studied polymers. Considering the fact that the monoclinic structure is usually metastable in nature that relaxes easily at ambient condition, this discovery is quite intriguing. In addition, we found that this conformation still existed in the films that were previously melted at 250 °C, which emphasizes its stability. The monoclinic structure may indicate that shear-induced crystallization occurred probably during a fabrication step of UHMWPE. An alternative explanation is the possible development of microstresses due to an extension of the molecular segments that are caused either by external deforming strains or by the

Table 3. Nonisothermal DSC Crystallization Properties Obtained Cooling from the Melt (200 °C) with the Cooling Rate of 10 °C/min

name	H_c (J/g)	slope[a] (W/g/°C)	T (°C) at the peak max	X_c (%)
1050	117.0	−0.362	114.5	40.5
1050-0	108.0	−0.325	114.0	37.5
1050-10	111.0	−0.166	114.0	38.5
1050-50	115.0	−0.143	117.0	40.0
1050-100	110.5	−0.130	120.5	38.5
1020	122.0	−0.356	115.5	42.0
1020-0	120.0	−0.401	115.0	41.5
1020-10	110.0	−0.230	115.5	38.5
1020-50	114.5	−0.160	115.5	40.0
1020-100	116.5	−0.163	119.5	40.5

[a] Initial slope of the crystallization exotherm.

Table 4. Nonisothermal DSC Crystallization Properties Obtained Cooling from the Melt for Nonirradiated and Irradiated (50 KGy) 1050 Samples with Different Cooling Rates

	1050-0		1050-50	
cooling rates (°C/min)	H_c (J/g)	slope (W/g/°C)	H_c (J/g)	slope (W/g/°C)
1	119.0	−0.155	117.0	−0.034
5	117.5	−0.311	116.0	−0.091
10	108.0	−0.325	115.0	−0.144
20	115.0	−0.330	115.0	−0.206

increase in size of crystallites during the annealing process. Relaxation of these microstresses is usually accompanied by polymorphous transitions from orthorhombic to a monoclinic crystal lattice during annealing, which have been discussed elsewhere.[8]

From the nonisothermal DSC data, summarized in Tables 3 and 4, we learned that approximately the same degree of crystallinity of UHMWPE (around 40%) could be attained regardless of irradiation dose or molecular weight used. Different cooling rates presented in Table 4 did not alter the crystallinity level either. A calculation of the initial slope of the crystallization exotherm was employed to express relative kinetics of these nonisothermal processes. Higher absolute values of the slope, suggesting faster crystallization, were assigned to the nonirradiated samples. With an increase in irradiation dose, nonisothermal crystallization rate apparently slowed. The cooling rate also had a profound effect on the crystallization kinetics, as indicated in Table 4. The crystallization was faster for higher cooling rates, suggesting the nucleation-dominated process. In addition, we detected a significant change in the peak width and the onset of crystallization during the control cooling steps from 200 °C, as shown in Figure 2. The onset of crystallization shifted to higher temperatures and the peak distribution increased systematically with irradiation dose, suggesting an increase in the distribution of crystal dimensions. These phenomena observed in irradiated samples were not affected by the cooling rate used. The information we have gathered indicates that this feature could be based upon the morphological changes developed during the irradiation process. This issue will be addressed in more detail later in the text.

2. Isothermal Crystallization Kinetics from DSC Measurements. DSC data for the isothermal melt crystallization of UHMWPE collected over the temperature range 110−124 °C are summarized in Table 5. Kinetic curves of the 1050-0 and 1050-50 samples fit very well to the classical Avrami equation,[23] with calculated values of the Avrami exponent, n, of about

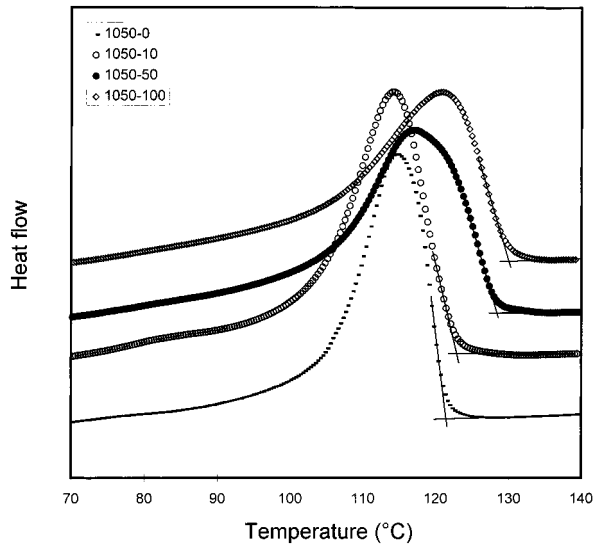

Figure 2. DSC traces obtained during nonisothermal crystallization of different 1050 samples with the cooling rate of 10 °C/min. Two upper graphs were shifted vertically for clarity reasons.

Table 5. Isothermal DSC Crystallization Properties of Nonirradiated and Irradiated (50 KGy) 1050 Samples Generated at Different Crystallization Temperatures

	1050-0			1050-50		
T (°C)	H_c (J/g)	$t_{1/2}$ (s)	n	H_c (J/g)	$t_{1/2}$ (s)	n
110	88.0	38	3.3	110.0	43	2.9
112	78.0	38	3.4	91.0	39	2.9
114	61.0	36	3.2	81.0	37	2.9
116	47.0	35	3.1	64.0	34	2.9
118	36.0	42	3.3	54.0	36	3.0
120	20.5	50	3.5	44.0	37	3.1
122	N/A[a]			34.5	37	3.2
124	N/A[a]			22.0	32	3.1

[a] There was an insufficient amount of crystallinity developed to perform accurate measurement.

3.3 and 3.0 for nonirradiated and samples irradiated at 50 KGy, respectively. Mandelkern and co-workers[24] reported $n = 3$ for the virgin fractionated UHMWPE in the molecular weight range from 1.95×10^4 to 8×10^5. Interestingly, they found that this value was reduced to $n = 2$ for the molecular weights greater than 8×10^5, indicating the growth habit changes from two-dimensional to one-dimensional. Although our nonirradiated polymers seem to belong to this category according to their average chain size, we did not detect such kinetics behavior. This could be due to the fact that UHMWPE used in this study was unfractionated; i.e., its molecular weight distribution was much broader than for the samples used by Mandelkern and others. Next, the crystallinity content, which was calculated from the DSC exotherms (the second column in Table 5), showed a systematic increase with the degree of undercooling. This feature may reflect nucleation-dominated crystallization with very limited crystal growth. Because of the very fast rate of nucleation (as indicated in the following section), the concentration of nuclei becomes so dense that there was not sufficient space for a subsequent lateral growth. Considering the extremely long macromolecular chains in UHMWPE, multiple nucleation of an individual chain is the one of the possible nucleation mechanisms for this process.

We will now focus on the half-time of crystallization, $t_{1/2}$, data presented in Table 5 for two types of UHMWPE films. Interestingly, relatively short $t_{1/2}$ values, which correspond to the fast rates, were found to be practically independent of crystallization temperature in the 110−124 °C range studied. This behavior is quite unusual and conflicts with the kinetics data obtained by Fatou et al.[24] on the fractionated UHMWPE over the temperature range from 114 to 128 °C. Using DSC methods, they observed a very profound temperature dependence on the crystallization rate. Values of $t_{1/2}$ gradually and substantially increased with an increase in crystallization temperature. We believe that the reason for the temperature-independent kinetics in our polymers is the presence of specific ordered domains preserved well above the melting point in both irradiated and nonirradiated UHMWPE. A detailed description of this phenomenon will be introduced in the next section by hot stage optical microscopy and depolarized light scattering data. In addition, for a given crystallization temperature, kinetics data of nonirradiated and irradiated polymers displayed in Table 5 were similar, except for the higher temperature region where higher levels of crystallization of the irradiated samples were achieved. This is in full agreement with our nonisothermal DSC results that were presented earlier in the text. We suspect that a new population of supposedly shorter chains was generated in UHMWPE during irradiation which start to crystallize at higher temperatures. However, inherent difficulties of recording the molecular weight distribution of the studied polymers prevented us of confirming this hypothesis.

3. UHMWPE Crystal Morphology As Revealed by Hot Stage Optical Microscopy and Depolarized Light Scattering. In this section we will discuss UHMWPE crystal morphology developed during melt quenched isothermal crystallization using hot stage optical microscopy (HSOM) and depolarized light scattering (DLS). The morphological forms obtained under controlled nonisothermal conditions were found to closely match those reported for isothermal crystallization and, hence, will not be presented here.

HSOM images captured during isothermal crystallization of nonirradiated UHMWPE (1050-0) at 120 °C as a function of time are shown in Figure 3a−d. A very characteristic pattern, which consists of a large number of spherulites organized in the ring structures, was observed. These supramolecular structures resemble, in a way, a honeycomb. Further crystal growth was carried out at the expense of these rings, as they served as effective nucleation sites. Thus, after a certain crystallization level was reached, clusters of spherulites became predominant crystal forms. Curiously, even after the polymer was melted at temperatures very close to the degradation point,[25] observed spherulite forms reappeared exactly at the same location every time. This very strong memory effect was unexpected and may arise due to an exceptionally low chain mobility of UHMWPE. An evidence of the similar type of memory effect for relating materials can be found in the literature. Barham,[26] for example, studied a matrix of linear polyethylene ($M_w = 40\,000$) and deuterated polyethylene (DPE) ($M_w = 119\,000$) using small-angle neutron scattering. The resulting material showed a high degree of extension of the high molecular weight DPE molecules, but the lower molecular weight polyethylene molecules lost their extension during relaxation process. The author suggested that the melting process of DPE could

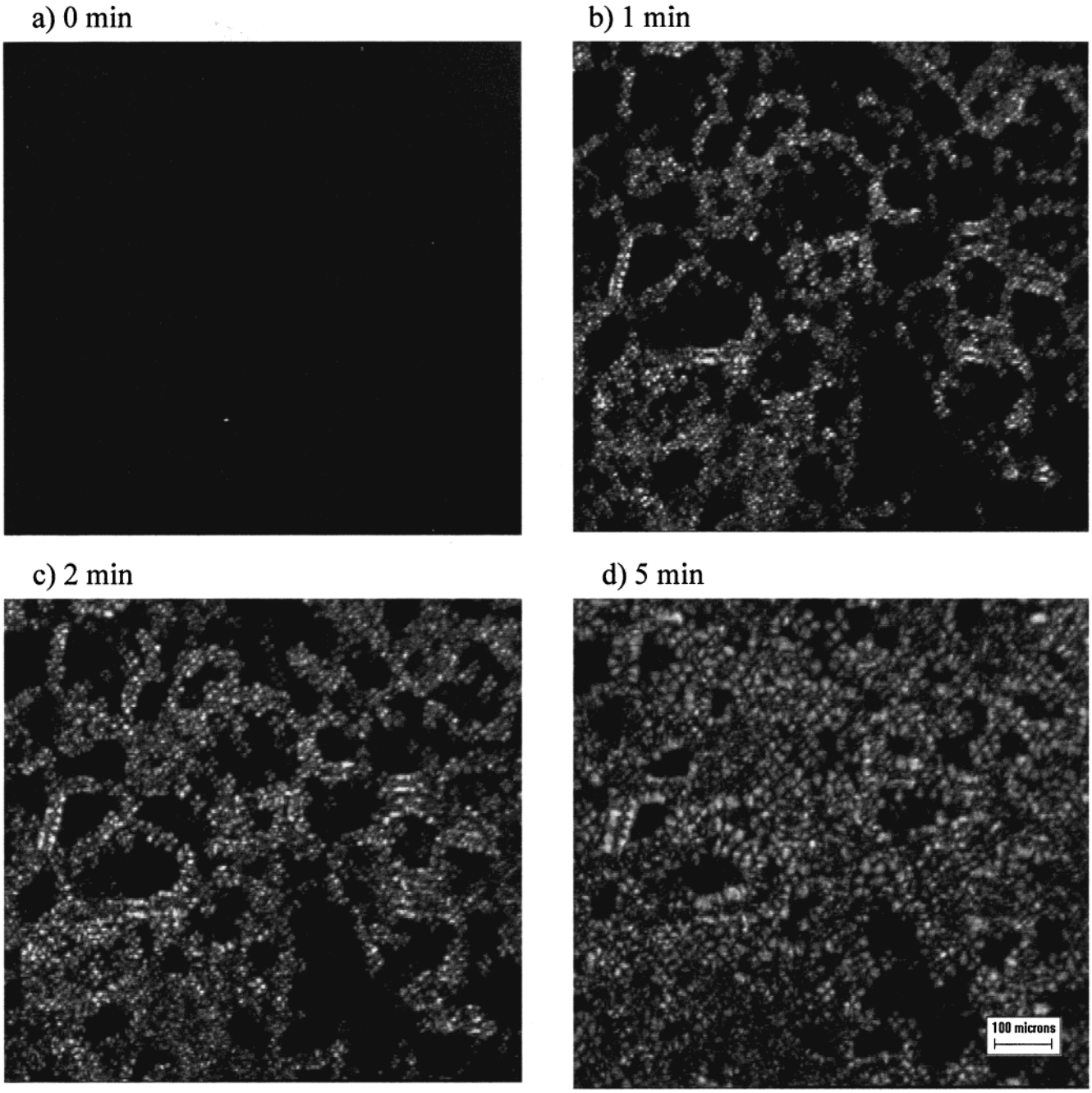

Figure 3. HSOM images of nonirradiated 1050 sample (thickness 0.1 mm) captured during isothermal crystallization at 120 °C after (a) 0, (b) 1, (c) 2, and (d) 5 min.

involve some sort of cooperative process throughout the crystals.

The characteristic "honeycomb" structures were also detected in HSOM images of the nonirradiated, lower molecular weight polymer (1020-0, thickness of 0.1 mm) captured under the same crystallization conditions. As indicated in Figure 4A, the nucleation density for this polymer seems to be higher, having spherulite clusters formed earlier in the process. HSOM images of the irradiated sample (1020-50) presented in Figure 4B contain a quite different morphology. From the very beginning of the process, relatively large (50−100 μm) rodlike ordered grains were found already existing in the system. Further crystallization proceeded on the skirt of these domains characterized by a faded non-spherulitic morphology. The similar type of crystal morphology was also observed for 1050-50 polymer, but due to a space confinement these data will not be displayed here. To provide an appropriate answer to what causes these different crystal formations, an optical analysis of the studied polymers in the melting state prior to crystallization is required. However, before turning the reader's attention to this subject, we would like to introduce depolarized light scattering (DLS) results that were generated on the same materials and conducted under the same experimental conditions.

DLS images of the nonirradiated (1050-0) and irradiated (1050-50) UHMWPE films, captured after 5 min of isothermal crystallization at 120 °C, are shown in Figure 5. A nonirradiated polymer film (Figure 5a) produced a regular four-lobe pattern characteristic for spherulite morphology accompanied by a small, relatively weak point light in the middle. The truncated cross pattern comes from the scattering of individual

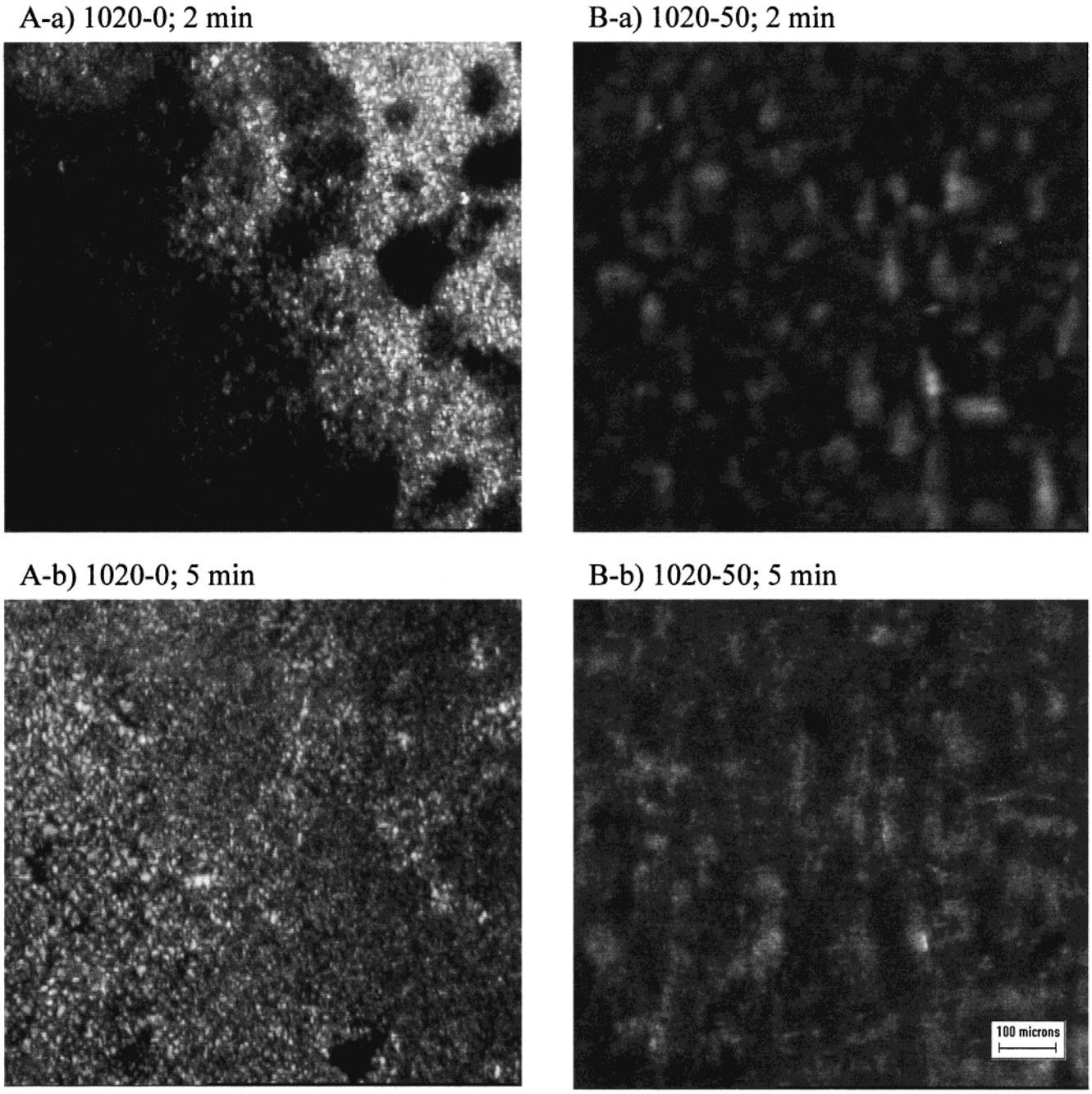

Figure 4. HSOM images of nonirradiated and irradiated (thickness 0.1 mm; 50 KGy) 1020 samples, captured during isothermal crystallization at 120 °C: (A) 1020-0, after (a) 2 and (b) 5 min; (B) 1020-50, after (a) 2 and (b) 5 min.

spherulites observed earlier in Figure 3. The center light belongs to the scattering of larger domains, in this case spherulite clusters, as its intensity was found gradually increasing with crystallization time. The crystallinity plateau was reached after about 5 min of the process, causing the image shown in Figure 5a to stop changing. At lower crystallization temperatures, both types of patterns became progressively more intense, indicating a higher crystallinity content. However, the signature of spherulite morphology is absent in the DLS images of the irradiated sample (1050-50), as shown in Figure 5b. We found that regardless of the molecular weight used, for all irradiated samples crystallized in the temperature range from 110 to 124 °C, only an azimuthally independent light scattering pattern was present. Those patterns can be attributed to the scattering of larger, randomly oriented crystalline domains, as seen before in HSOM images of the 1020-50 polymer (Figure 4B). In addition, the truncated crosses were also observed for the scattering of the nonirradiated 1020-0 polymer as shown in Figure 6a−c. In comparison with the corresponding images of the 1050-0 sample, these lobes appeared considerably smaller, suggesting that the scattering could arise from a larger spherulite-type structure. This structure may have a spherulite cluster form, which was found to accompany crystallization from the very early stages of the process (see Figure 4A). Nonspherulitic morphology of the irradiated 1020-50 sample was manifested in Figure 6d by the absence of four-lobe symmetry. Manderkern and others,[27,28] on the other hand, reported that DLS patterns of fractionated polyethylenes were strongly affected by their molecular weights (MW). For the intermediate MW zone (from 9×10^5 to about 3×10^6), they discovered the

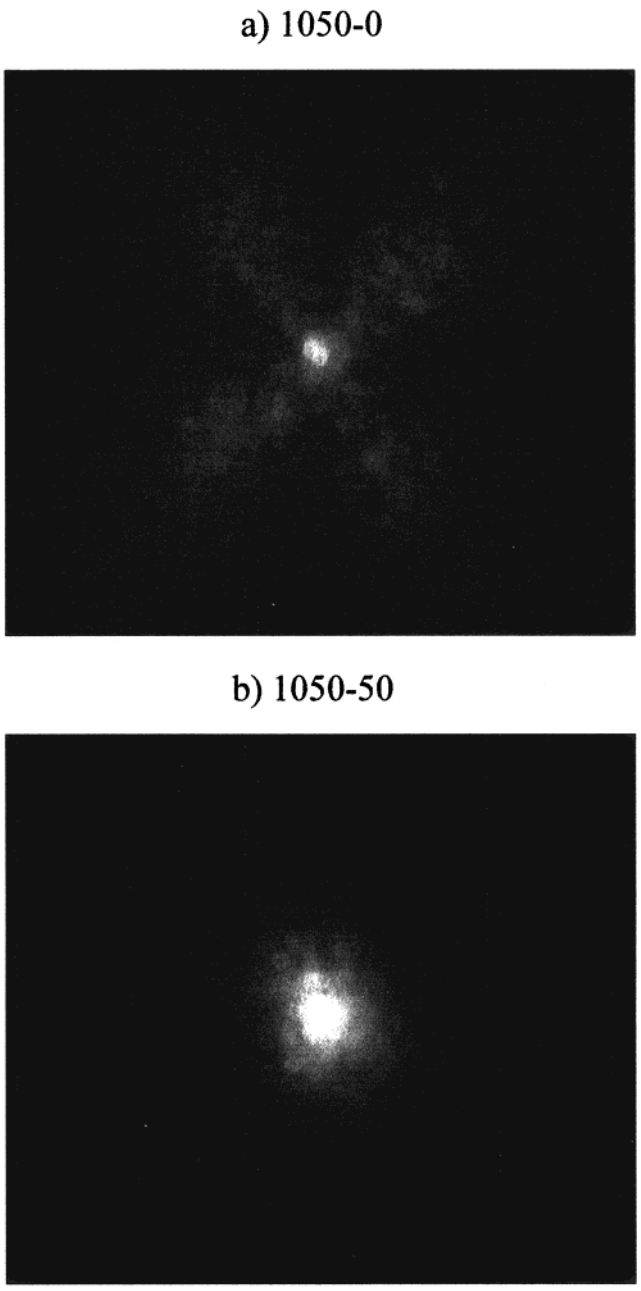

Figure 5. DLS images of nonirradiated and irradiated (thickness 0.1 mm; 50 KGy) 1050 samples, captured during isothermal crystallization at 120 °C after 5 min: (a) 1050-0 and (b) 1050-50.

specific crystallization temperature (T_{sp}) at which the scattering pattern changes from spherulitic to nonspherulitic kind. For molecular weights under 9×10^5 only regular spherulites were found, while those above 3 million contained an azimuthally independent light scattering pattern, indicating the random oriented lamellae.

Finally, the resultant melt morphology of the UHMWPE films was examined after the samples were isothermally heated at temperatures up to 250 °C. Measurements at higher temperatures were prevented by the occurrence of a color change from white to brownish that sets in at about 255 °C, which indicates the onset of oxidation/degradation processes. The thermal degradation study of this polymer was conducted previously in the range between 284 and 355 °C and found to proceed by a typical random scission type reactions.[25] HSOM images of the nonirradiated UHMWPE film and those irradiated to different doses, captured after 5 min of the isothermal treatment at 250 °C, are shown in Figure 7a−d. The optical image of the nonirradiated polymer was characterized by, apparently, a complete melting of the crystal structures, which were developed during an annealing process. However, a drastic change in optical images was detected between nonirradiated and irradiated samples. Images in Figures 7b−d suggest a presence of ordered structures that exist, quite surprisingly, well above the polymer's melting point. Interestingly, the size of these domains seems to decrease systematically with an increase in irradiation dose. The tendency in grain shape was also found to change with irradiation dose: from a large extended region observed for the 1050-10 sample to smaller predominantly oval domains (average size 30−50 μm) obtained from the polymer irradiated to the highest dose. Corresponding DLS images of UHMWPE films (not shown here), captured under the same melt conditions, indicated superb agreement with our optical microscopy data. With an increase in irradiation level, the size of oval azimuthally independent patterns gradually increased, confirming an observed decrease in the size of ordered domains as presented by optical microscopy data.

The issue to be addressed here is what causes these structures to preserve their conformations even after being heated at such high temperatures. The first possibility is that observed structures were never changed too much from their original positions occupied during polymerization; the overall chain location remain unchanged even after melting, which was seen in the micrographs taken at 250 °C (Figure 7). The other possibility is that a presence of stable monoclinic structure in our polymers, suggested previously by WAXD data (Figure 1), probably originated from one or more manufacturing steps performed at high temperatures. Murase et al.[29] reported fairly similar behavior of UHMWPE in paraffin solution by detecting the "butterfly pattern" under the nonquiescent experimental conditions at temperatures higher than equilibrium melting point. They observed the signature of shear-induced concentration fluctuations or phase separation process using the shear small-angle light scattering and shear optical microscopy. Second, it was also suggested[30,31] that the lamellar structure of UHMWPE contains a high concentration of entangled tie macromolecules in the amorphous region. During the melting process, the physical net of stable entanglements that is formed may hinder the conformational transitions of the macromolecular chains from crystal into amorphous phase. Obviously, this effect can be more pronounced for the irradiated samples, where the cross-linking density additionally slows diffusion of chains in the polymer. Besides, we believe that the described ordered domains in the melt directly influenced the crystallization kinetics of UHMWPE. These structures served as preexisting nucleation cites for the chain-type progressive nucleation facilitated at the lower crystallization temperatures. Because of an early crystal impingement, very limited crystal growth was observed in most of the samples, causing the crystallization rate of the isothermal process to be controlled only by nucleation rate. Since the nucleation phenomenon was found to be closely related to the preexistence of ordered grains (note that even in the nonirradiated sample a strong

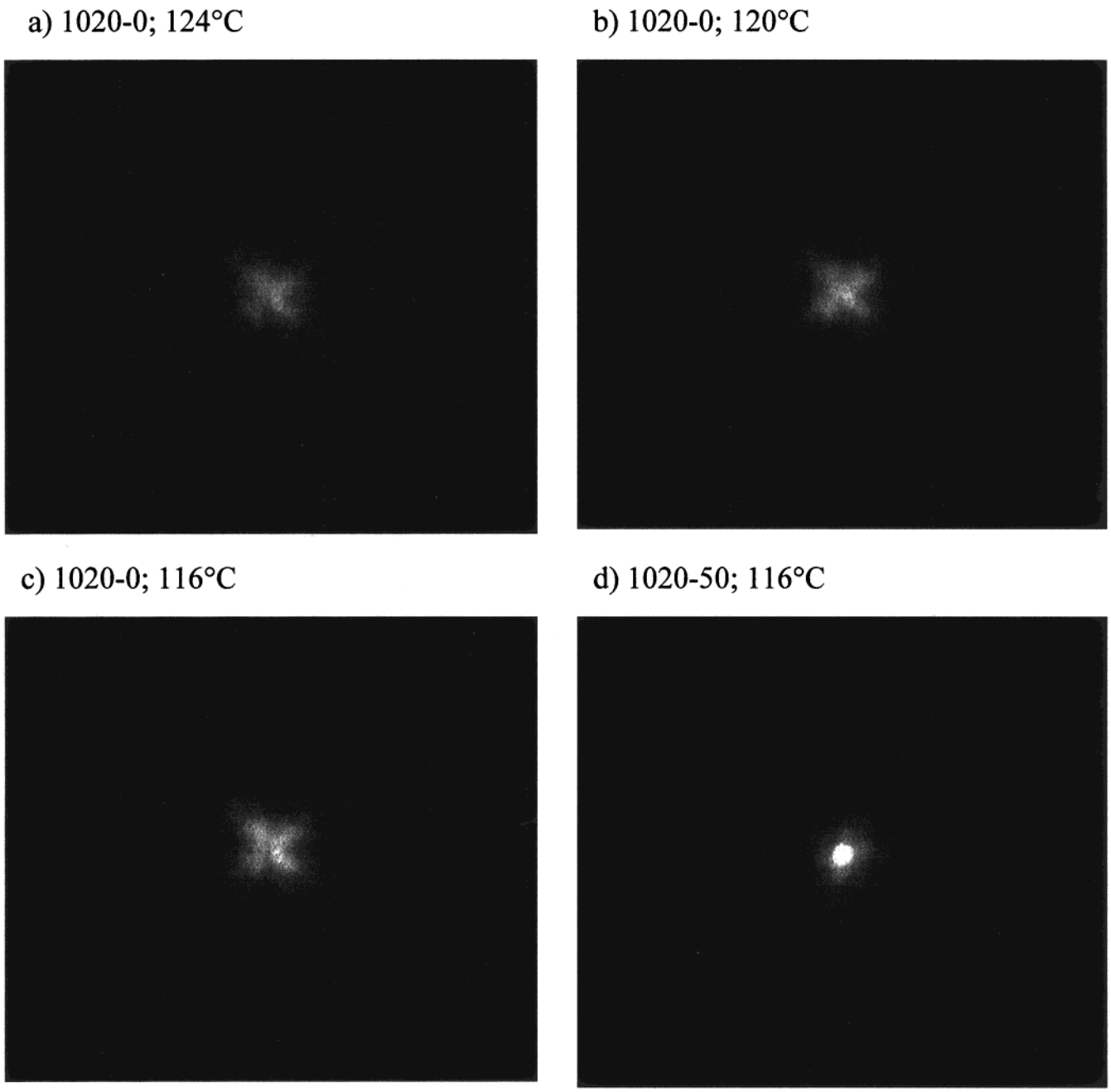

Figure 6. DLS images of nonirradiated and irradiated (thickness 0.1 mm; 50 KGy) 1020 samples, captured during isothermal crystallization runs conducted at different temperatures after 15 min: (a) 1020-0, at 124 °C; (b) 1020-0, at 120 °C; (c) 1020-0, at 116 °C; and (d) 1020-50, at 116 °C.

memory effect was observed), the overall crystallization kinetics of UHMWPE become practically independent of temperature. On the other hand, during nonisothermal crystallization runs conducted under control cooling rates, a larger ordered domains detected in the irradiated samples might provide a rationale for the premature crystallization as indicated in Figure 2.

Conclusions

Crystallization kinetics and resultant morphology of ultrahigh molecular weight polyethylene (UHMWPE) were examined after the polymer had been subjected to γ-irradiation (10−100 KGy) in a vacuum. Differential scanning calorimetry (DSC) and wide-angle X-ray diffraction (WAXD) were used to gain information about crystalline state of nonirradiated and irradiated UHMWPE films from the two molecular weight series: 3 million (1020) and 6 million (1050). The degree of crystallization decreased with irradiation dose at the same rate for both groups. The largest drop in crystallinity was detected in the lowest irradiation dosed (10 KGy) samples. This can be explained by the network formation that apparently prevailed over chain scission processes in the irradiated UHMWPE samples, lowering the crystallinity due to imposed geometrical constrains. Furthermore, WAXD patterns indicated a substantial amount of stable monoclinic structure observed for all studied polymers. This conformation probably originated either from the polymerization process or from induced stresses that occurred during different fabrication steps of UHMWPE at high temperatures. From the nonisothermal DSC measurements, we detected a sig-

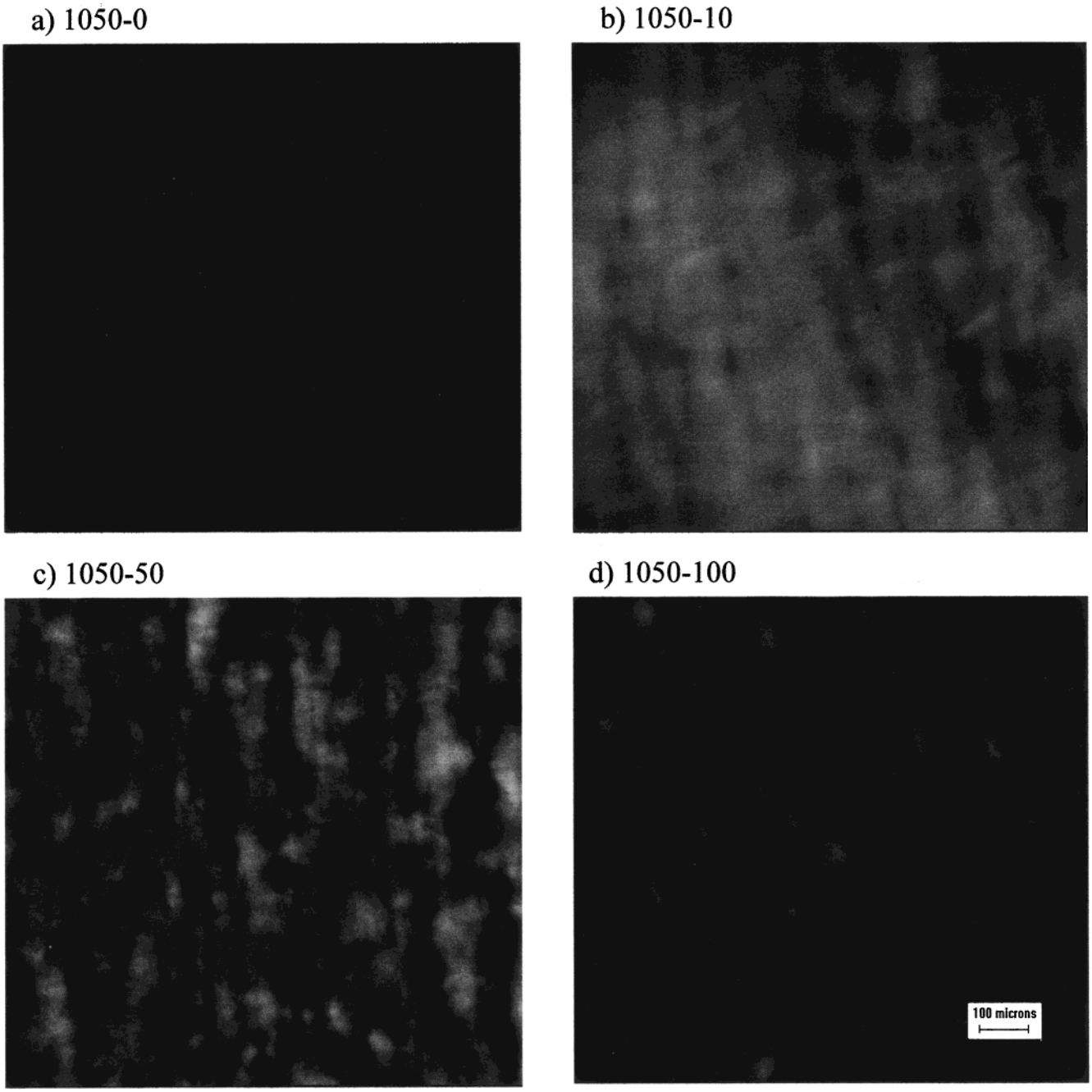

Figure 7. HSOM images of nonirradiated and irradiated 0.1 mm thick 1050 samples, captured during isothermal heating at 250 °C after 5 min: (a) 1050-0, (b) 1050-10, (c) 1050-50, and (d) 1050-100.

nificant gradual change in the onset of crystallization with irradiation. During the controlled cooling from the melt, samples irradiated to higher dose experienced crystallization earlier; i.e., the onset was shifted to higher temperatures.

DSC kinetics curves obtained from the isothermal crystallization of UHMWPE fit very well to the classical Avrami equation, with calculated Avrami exponents, n, of 3.0 and 3.3 for nonirradiated and irradiated samples, respectively. The analysis of crystallization exotherms revealed a substantial but gradual increase in crystallinity with a decrease in crystallization temperatures, reflecting a nucleation-dominated process. However, values of the crystallization half-time, $t_{1/2}$, were found to be practically independent of both temperature and irradiation dose. This phenomenon was connected to the presence of stable ordered grains which did not "melt" even after being subjected to extreme temperatures. At lower temperatures, progressive chainlike nucleation proceeded right on the skirt of these domains, maintaining the constant crystallization rate regardless of the degree of undercooling.

Supramolecular crystal morphology of UHMWPE films was also found to be strongly affected by irradiation level as seen by hot stage optical microscopy (HSOM) and depolarized light scattering (DLS). A large number of spherulites organized in ring structures ("honeycomb") were detected in HSOM images of the nonirradiated samples captured during isothermal crystallization. The nucleation rate of the lower molecular weight UHMWPE (1020) was apparently higher, as the spherulite cluster formation accompanied the very early stages of the crystallization process. Consequently, corresponding DLS images of this polymer contained the

four-lobe pattern of a considerably smaller size, suggesting that in this case the scattering pattern may originate from clusters of spherulites. On the other hand, HSOM and DLS images of irradiated samples showed an absence of any ordered supramolecular structures. Faded nonspherulite morphology with larger grains observed by HSOM was confirmed by azimuthally independent DLS patterns. In addition, an average size of the larger ordered domains was found to gradually decrease with an increase in irradiation dose. These unique features of irradiated UHMWPE can be attributed to the exceptionally slow diffusion of chains in the polymer, caused by the physical net of stable entanglements and enhanced by the extensive cross-linking produced by γ-irradiation, which hindered the conformational transitions of the macromolecules from crystal into amorphous phase.

Acknowledgment. This work was supported by a Johnson & Johnson Corporate Office of Science and Technology (COSAT) Excellence in Science Award Grant. The authors thank Dennis Jamiolkowski and Edward Dormier of Ethicon, Inc., for their support and valuable discussions of the manuscript. We are also very grateful to Prof. Benjamin Hsiao and Shaofeng Ran of New York State University at Stony Brook for their assistance with the SAXS experiments at Brookhaven National Laboratory.

References and Notes

(1) Harris, W. *Acta Orthop. Scand.* **1994**, *65*, 113.
(2) Goldman, M.; Pruitt, L. *J. Biomed. Mater. Res.* **1998**, *40*, 378.
(3) Muratogly, O. K.; Bragdon, C. R.; O'Connor, D. O.; Jasty, M.; Gul, R.; Harris, W. H. *Polym. Mater. Sci. Eng.* **1998**, *79*, 498.
(4) Kurtz, S.; Muraloglu, O.; Evans, M.; Edidin, A. *Biomaterials* **1999**, *20*, 1659.
(5) McKellop, H.; Shen, F.; Lu, B.; Campbell, P.; Solovey, R. *J. Orthop. Res.* **1999**, *17*, 157.
(6) Spiegelberg, S. H.; Kurtz, S. M.; Edidin, A. A. 1999 Society for Biomaterials, 25th Annual Meeting Transactions, p 215.
(7) Flory, P. J. *Principles of Polymer Chemistry*; Cornell University Press: Ithaca, NY, 1953.
(8) Mandelkern, L. *Crystallization of Polymers*; McGraw-Hill: New York, 1963.
(9) Andjelić, S.; Jamiolkowski, D. D.; McDivitt, J.; Fischer, J.; Zhou, J., submitted to *J. Polym. Sci. Phys. Ed.*
(10) Dai, H. J. Ph.D. Dissertation Thesis, Polytechnic University, New York, June 1998.
(11) Hsiao, B. S.; Verma, R. K. *J. Synchrotron Radiat.* **1998**, *5*, 23.
(12) Wang, Z. G.; Hsiao, B. S.; Zong, X. H.; Yeh, F.; Dormier, E.; Jamiolkowski, D. D. *Polymer* **2000**, *41*, 621.
(13) Andjelić, S.; Jamiolkowski, D. D.; McDivitt, J.; Fischer, J.; Zhou, J.; Wang, Z.; Hsiao, B. S. *J. Polym. Sci., Phys. Ed.* **2001**, *39*, 153.
(14) Choundhury, M.; Hutchings, I. M. *Wear* **1997**, *203−204*, 335.
(15) Deng, M.; Shalaby, W. S. *J. Appl. Polym. Sci.* **1995**, *58*, 2111.
(16) Kamel, J.; Finegold, L. *J. Polym. Sci., Phys. Ed.* **1985**, *23*, 2407.
(17) Bhateja, S. K. *Polymer* **1982**, *23*, 654.
(18) Ikada, Y.; Nakamura, K.; Ogata, S.; Makino, K.; Tajima, K.; Endoh, N.; Hayashi, K.; Fujita, S.; Fujisawa, A.; Masuda, S.; Oonishi, H. *J. Polym. Sci., Chem. Ed.* **1999**, *37*, 159.
(19) Hoffman, J. D.; Davis, G. T. *Treatise on Solid State Chemistry*; Plenum Press: New York, 1976; Vol. 13.
(20) Wunderlich, B. *Macromolecular Physics*; Academic Press: New York, 1973; Vol. 1.
(21) One way to confirm the crystal nature of these ordered domains, observed in our laboratory by HSOM and DLS techniques, is to perform synchrotron WAXD experiments at the temperatures much higher than the regular "melting points" of these materials. We hope that in the future we will be able to perform this kind of measurement.
(22) Bellare, A.; Schnablegger, H.; Cohen, R. E. *Macromolecules* **1995**, *28*, 7585.
(23) Avrami, M. *J. Chem. Phys.* **1940**, *8*, 212.
(24) Fatou, J. G.; Marco, C.; Mandelkern, L. *Polymer* **1990**, *31*, 1685.
(25) Kuroki, T.; Sawaguchi, T.; Niikuni, S.; Ikemura, T. *Macromolecules* **1982**, *15*, 1460.
(26) Barham, P. J. In *Crystallization of Polymers*; Dosière, M., Ed.; NATO ASI Ser., Ser. C; Kluwer Academic Pub.: Dordrecht, 1993; Vol. 405, pp 153−158.
(27) Mandelkern, L.; Glotin, M.; Benson, R. A. *Macromolecules* **1981**, *14*, 22.
(28) Maxfield, J.; Mandelkern, L. *Macromolecules* **1977**, *10*, 1141.
(29) Murase, H.; Kume, T.; Hashimoto, T.; Ohta, Y.; Mizukami, T. *Macromolecules* **1995**, *28*, 7724.
(30) Kresteva, M.; Nedkov, E.; Radilova, A. *Colloid Polym. Sci.* **1985**, *263*, 273.
(31) Minkova, L. *Colloid Polym. Sci.* **1988**, *266*, 6.

MA0008241